Earth and Planetary Science Letters 511 (2019) 89–98

Contents lists available at ScienceDirect

Earth and Planetary Science Letters

www.elsevier.com/locate/epsl

Role of ancient, ultra-depleted mantle in Mid-Ocean-Ridge magmatism

A. Sanfilippo [a,b,*], V. Salters [c], R. Tribuzio [a,b], A. Zanetti [b]

[a] Dipartimento di Scienze della Terra e dell'Ambiente, Università degli Studi di Pavia, Via Ferrata 1, Pavia, Italy
[b] CNR – Istituto Geoscienze e Georisorse, U.O., Pavia, Via Ferrata 1, Pavia, Italy
[c] Dep. of Earth, Ocean and Atmospheric Science and National High Magnetic Field Laboratory, Florida State University, Tallahassee, FL, USA

ARTICLE INFO

Article history:
Received 2 August 2018
Received in revised form 22 December 2018
Accepted 11 January 2019
Available online 5 February 2019
Editor: F. Moynier

Keywords:
Hf–Nd isotopes
mantle peridotite
melt-rock reaction
MORB
Lanzo Massif

ABSTRACT

There is debate to what degree mid-ocean ridge basalts (MORB) can be used to infer the composition of the sub-ridge mantle and whether the upper mantle contains components that are difficult to recognize by observations on MORB alone. Here we report trace element and isotope data on a fossil mantle section exposed in the ophiolitic Lanzo South massif, Italy. Our findings show the existence of clinopyroxenes in geochemically depleted melt-infiltrated harzburgites with an extreme radiogenic Hf-isotopic composition but MORB-like Nd isotopic compositions. The simplest way of explaining the depleted trace elements in combination with the decoupled isotopic compositions is that the harzburgites were infiltrated by a melt with isotopic compositions inherited from an anciently (>1 Ga) depleted source. The existence of melts from ultra-depleted sectors of the asthenosphere allows constraining of the configuration of the heterogeneities in the sub-ridge mantle. The parallel arrays in Hf–Nd isotope composition space of different Mid-Ocean ridge segments imply the ubiquitous presence of anciently depleted residual mantle as the matrix in which more enriched components occur in pockets.

1. Introduction

The compositional heterogeneity of the Earth's mantle has mainly been studied through basalts erupted on the surface. Different mantle components are distinguished by the identification of difference in the isotopic signature in basalts, which in turn are associated with specific mantle materials (Zindler and Hart, 1986; Stracke, 2012). One of these mantle materials is incompatible element depleted residual peridotite (so called *DM*), left behind after melting of the shallow mantle (Hofmann, 1997). Incompatible element enriched reservoirs are produced by large-scale cycling of chemical components between the continental and oceanic crust or lithosphere and the upper mantle (White and Hofmann, 1982). The DM is preferentially sampled by Mid Ocean Ridge Basalt (MORB). The most depleted MORB samples ($\varepsilon_{Nd} \sim +10$–$+14$) are commonly thought to directly reflect the isotopic composition of the DM, which is a key parameter for reconstructing the long-term chemical evolution and estimating the relative mass of the depleted upper mantle (Allegre et al., 1984; Salters and Stracke, 2004).

Although the existing Nd isotope data on clinopyroxene (cpx) from abyssal peridotites overlap the isotopic composition of MORB (Snow et al., 1994; Salters and Dick, 2002; Cipriani et al., 2004; Warren et al., 2009), a significant number of them extend to higher values (Stracke et al., 2011; Cipriani et al., 2011; Mallick et al., 2014; Byerly and Lassiter, 2014). Abyssal peridotites thus seem to reflect a slightly greater extent of mantle depletion than MORB (ε_{Nd} for peridotites up to $+21$ versus ε_{Nd} for MORB up to $+14$). Hf isotopes further validate this hypothesis, showing that although the isotopic composition of the abyssal peridotites is mostly concentrated in the depleted part of the global MORB field ($\varepsilon_{Hf} = 10$–30), a growing number samples reveal more radiogenic compositions (ε_{Hf} up to $+300$) (Fig. 1; Stracke et al., 2011; Salters and Dick, 2011; Mallick et al., 2014; Byerly and Lassiter, 2014). Likewise, the occurrence of depleted $^{187}Os/^{188}Os$ ratios in abyssal peridotites also reflect long-term preservation of refractory (or ultra-depleted) domains (Alard et al., 2005; Liu et al., 2008). Portions of the asthenospheric mantle formed as ancient, lithospheric melting residues (called ReLish for Refractory Lithosphere), are preserved during the long term-advection and re-homogenization in the mantle (Salters et al., 2011). Owing to their depleted compositions these ultra-depleted domains were initially considered too refractory to melt in the shallow upper mantle under ocean ridges (Liu et al., 2008; Stracke, 2012), giving an elegant explanation of why these values are never found in the oceanic basalts. However, critical observations on a large number of Nd–

* Corresponding author at: Dipartimento di Scienze della Terra e dell'Ambiente, Università degli Studi di Pavia, Via A. Ferrata 1, I-27100, Pavia, Italy.
E-mail address: alessio.sanfilippo@unipv.it (A. Sanfilippo).

https://doi.org/10.1016/j.epsl.2019.01.018
0012-821X/

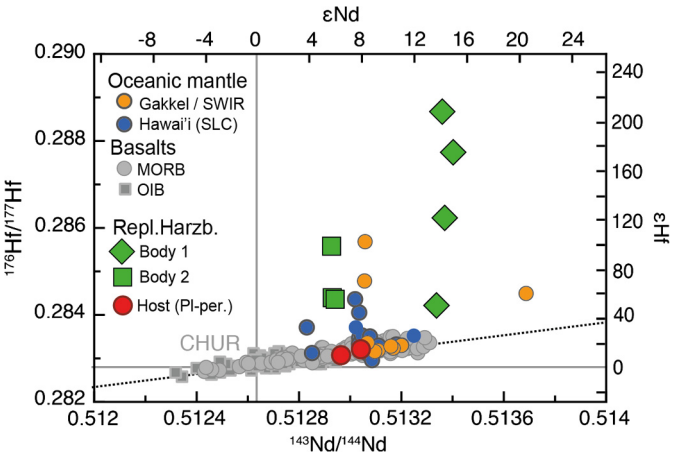

Fig. 1. Initial Hf and Nd isotope ratios of clinopyroxene from replacive harzburgites and host-peridotites (values recalculated at 160 Ma) compared to clinopyroxene from abyssal peridotites and whole-rock compositions of oceanic basalts (errors bars smaller than symbols size; see Table S4). The Hf and Nd isotope ratios of the peridotites from Gakkel Ridge (Stracke et al., 2011) and Salt Lake Crater xenoliths (Bizimis et al., 2003) range to both higher Hf and Nd isotope ratios compared to oceanic basalts. Note that the host Pl-peridotites from Lanzo plot in the field defined by MORB and by the Indian Ocean peridotites whereas the two replacive harzburgites bodies have Nd and Hf isotopes highly decoupled, with initial Nd isotopic ratios plotting in the MORB field and Hf extending towards the most radiogenic values documented so far. Samples from the two harzburgites bodies have highly variable Hf isotope ratios but nearly constant initial Nd isotope ratios. (For interpretation of the colors in the figure(s), the reader is referred to the web version of this article.)

Hf isotopic compositions of MORB challenge this idea and argue for the occurrence of a highly depleted, ancient component in the MORB mantle, unrecognizable by the Sr–Nd–Pb isotope systems alone (Salters et al., 2011).

Abyssal peridotites show that mantle melting is a near fractional process (Johnson et al., 1990) and produces primary mantle melts with different compositions. Although in rare instances primitive melts are retained in melt inclusions (Sobolev and Shimizu, 1993), most of the mantle melts are mixed prior to eruption, erasing some of the compositional heterogeneity of the source material. Geochemical models corroborate these observations and suggest that the depth and physical mechanism of melt migration fundamentally influence the trace element and isotope ratios of the erupted melts (Shorttle and Maclennan, 2011; Stracke, 2012; Rudge et al., 2013). The prevailing view is that melt extraction and magma migration occur in spatially confined high permeability channels (Quick, 1981). These channels are thought to form by a positive feedback between melt-flux, dissolution and reprecipitation, and are found in spatially defined replacive mantle bodies in the geological record (Kelemen et al., 1995). Such lithospheric melt migration channels may record a greater range of melt compositions than the aggregated melts erupted on the ocean floor.

Here, we argue that the trace elements and Hf- and Nd isotopic compositions of large replacive bodies exposed within the Lanzo ophiolite, in the Western Italian Alps, document melts from an ancient, ultra-depleted mantle. Based on the idea that such melts can be produced at Mid Ocean Ridge settings we suggest that the anciently depleted residual mantle is an ubiquitous component in the asthenosphere, constituting the matrix in which variably enriched components occur in pockets.

2. The Lanzo peridotite, previous work

The Lanzo ophiolite was exhumed during the opening of the Ligurian Thethys Ocean in the Middle Jurassic (Boudier and Nicolas, 1977) and represents a mantle sequence modified by migration of melts akin modern MORB (Müntener et al., 2005; Piccardo et al., 2007). The sequence was involved in the Alpine orogeny, as shown by local development of antigorite-serpentinites associated with eclogitization of gabbroic intrusions. Peak metamorphic conditions were estimated at 2.0–2.5 GPa and 550–620 °C (Pelletier and Müntener, 2006) in Eocene times.

The Northern and Central portions of Lanzo have a subcontinental character defined by radiogenic Nd–Hf isotope ratios and fertile compositions (Bodinier et al., 1991; Guarnieri et al., 2012). The Southern portion of the Lanzo ophiolite records a complex history of interaction between a depleted spinel-facies mantle protolith and migrating MORB-type melts produced by asthenospheric upwelling in conjunction with the opening of the nascent oceanic basin (Müntener et al., 2005; Piccardo et al., 2007). These peridotites typically show crystallization of magmatic plagioclase and/or pyroxene within the pre-existing peridotite minerals and mostly consist of plagioclase (pl)-bearing harzburgites to cpx-poor lherzolites. Spinel (spl) in the Pl-peridotites has Cr#[Cr/(Cr + Al)] (40–50 mol%) and TiO_2 contents (0.6–1.1 wt%) plotting in the field of the pl-bearing abyssal peridotites (Piccardo et al., 2007; Sanfilippo et al., 2014). Cpx is variably LREE-depleted and has heterogeneous Nd–Sr isotopic compositions that generally plot in the field of modern MORB (Bodinier et al., 1991). These compositions indicate that the melt-peridotite reaction event led to a chemical refertilization of the peridotite, thereby erasing the original geochemical signature of the spinel-facies mantle protolith and producing mineralogical, chemical and isotopic heterogeneity (see also Sanfilippo et al., 2014). The melt-peridotite event forming the Pl-peridotites was followed by formation of large replacive mantle bodies and by intrusion of MORB-like gabbro dykelets and dykes showing diffuse to sharp contacts with respect to the host rocks. U–Pb ages of zircons in some of these gabbros yield 158 to 163 Ma ages (Kaczmarek et al., 2008), which allowed constraining the timing of the migration event in the middle Jurassic. To sustain this idea, McCarthy and Müntener (2015) proposed that the spl-protolith of the Lanzo Pl-peridotite experienced partial melting at 273 ± 24 Ma. Hence, the Lanzo South sequence may represent a refertilized portion of a lithospheric mantle, intruded and modified by interactions with MORB-like melts during opening of a Jurassic embryonic ocean (see Picazo et al., 2016 for a review).

2.1. Replacive mantle bodies from Lanzo South

Large replacive dunite bodies are characteristic of the Southern portion of the Lanzo massif. These dunite bodies are tens of meters in scale and oriented parallel to the main foliation in the peridotite body (Boudier and Nicolas, 1977). The high forsterite content of olivine (ol) (Fo 89–90) coupled with high Cr# (35–45 mol%) and TiO_2 concentrations (0.3–0.6 wt%) of spl originated through interaction between the host peridotites and a migrating melt. In particular, cpx and ol incompatible trace element compositions suggest that these dunite bodies formed by the migration of melts with a MORB signature, although slightly enriched in LREE compared to N-MORB (Müntener et al., 2005; Piccardo et al., 2007; Sanfilippo et al., 2017). A second generation of replacive bodies occurs in Lanzo South. These replacive bodies are mainly discordant to the main foliation in the host Pl-peridotites and consist of geochemically depleted spl-harzburgites (Piccardo et al., 2007). The harzburgites have spl with on average somewhat lower TiO_2 contents and Cr# than the spl from pl-peridotites, and the REE patterns in the cpx more depleted but less fractionated than those from the pl-peridotite (Piccardo et al., 2007). In this study, we focus on this second generation of replacive rocks, reporting geochemical and isotope data obtained from two distinct spl-harburgite bodies.

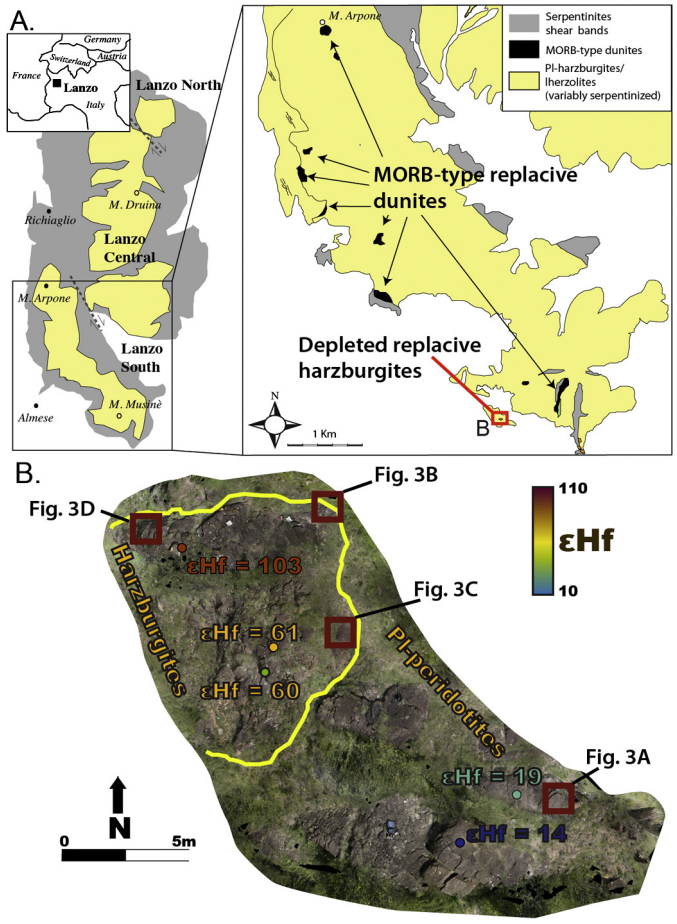

Fig. 2. Location and field occurrence of the studied harzburgite bodies. A) Schematic geological map and geographic location of the Lanzo Massif (redrawn from Boudier and Nicolas, 1977), with the location of the two replacive hazrburgites bodies. The replacive dunites with enriched to transitional MORB-type signature is also indicated. B) Ortho-rectified image of replacive harzburgite body 2 (8 mm/pixel) including the location of 3 harzburgite and 2 Pl-peridotite samples and respective εHf composition. The ortho-rectification of the image is based on 3-D model developed using the structure-from-motion technique on the basis of ~100 pictures (N. Menegoni, PhD thesis, University of Pavia). The location of Figs. 3A, 3B, 3C and 3D show the field occurrence of the harzburgites, contact zone and of the host Pl-peridotites. Note that the gradual disappearance of the foliation from the host peridotites, towards the contact. The replacive harzburgites do not show any fabric, in agreement with their replacive origin.

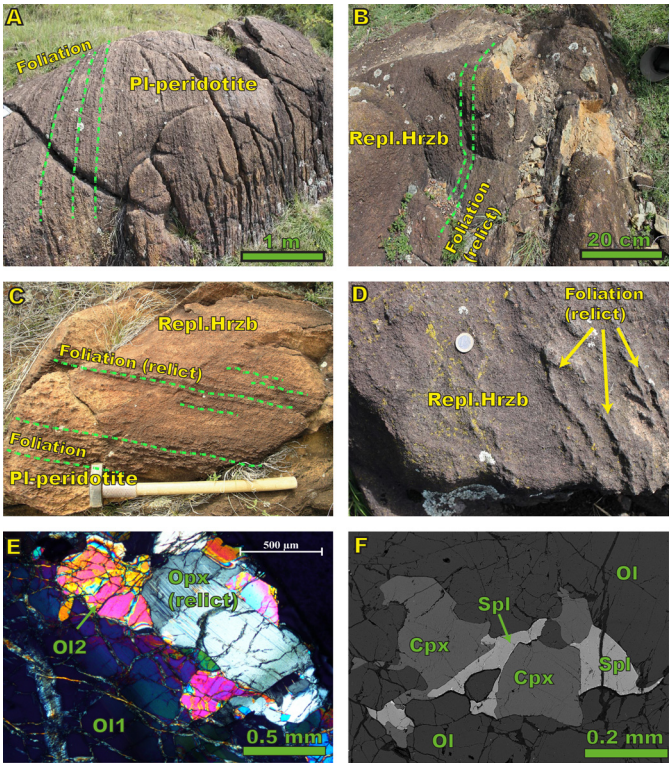

Fig. 3. Field and textural features of the Lanzo South replacive harzburgites and host Pl-peridotites. A) Foliation in the host Pl-peridotites defined by the occurrence of elongated pyroxene-rich and pyroxene-poor bands. B, C and D) Details of the contact between the replacive harzburgite body and the host Pl-peridotites. Relicts of the original foliation are still visible in the proximity of the contact and disappear completely within the replacive harzburgites. E) Large and kinked orthopyroxene (Opx) and olivine (Ol 1) porphyroclasts locally replaced by unstrained olivine (Ol2) in a replacive harzburgite (LZ30). F) Interstitial clinopyroxene (Cpx) and associated Cr-spinel (Spl) (Cr# = 25) within a replacive harzburgite (LZ205) indicating the crystallization of Cpx and Spl during the last phases of the replacive processes.

3. Sample selection and analytical techniques

3.1. Sample selection

Seven spl-harzburgites from two different replacive bodies were selected for this study. Selected spl-harzburgite bodies are up to 50 m in thickness and have a channel-like shape with nearly elliptical cross-sections (Fig. 2) and are located at a distance of ~200 m from each other. We also selected two host Pl-peridotites located at few meters from one of the two replacive bodies, where the contacts with replacive rocks are well exposed (Fig. 2B). In the field, the spl-harzburgites do not show any visible trace of foliation, thereby showing that the annealing of the original texture and consequent disruption of the foliated fabric constrained the formation of these replacive rocks (Figs. 3A to 3D). Olivine (Ol) in the replacive harzburgites range from large, kinked porphyroclasts to small, undeformed grains. Orthopyroxene (opx) is present as sub-rounded porphyroclasts, commonly kinked and showing lobate grain boundaries against the ol, indicative of a process of partial dissolution (Fig. 3E). Cpx is mostly found as undeformed, small (<0.2 mm) grains with interstitial habits. Anhedral Spl is often associated with the interstitial Cpx (Fig. 3F; see details of the textures in supplementary Table S1). Among the selected spl-harburgites, two samples still have trace amount of Pl, in the form of small (<0.05 mm), irregular grains not visible on the hand specimen. Plagioclase in these samples was likely inherited from the incomplete dissolution of the host rock (see discussion).

3.2. Major element whole-rock and mineral determinations

Whole-rock major element analyses (supplementary Table S2) were carried out by inductively coupled plasma atomic emission spectroscopy. Three blanks and five controls (three before sample group and two after) were analyzed per group of samples. Detection limits and values for standard material during the analyses are reported in Table S6. Precision and accuracy are estimated to be better than 2%. Major element compositions of minerals (supplementary Table S2) were achieved using a JEOL JXA-8200 electron microprobe located at Dipartimento di Scienze della Terra, Università degli Studi di Milano (Italy). Conditions of analyses were 15 kV accelerating voltage and 15 nA beam current. Counting time was 30 s on the peak and 10 s on the backgrounds. Natural standards were utilized and data reduction was carried out using the CITZAF package.

3.3. Trace element mineral determinations

Trace element compositions of olivine, clinopyroxene and orthopyroxene (supplementary Table S3) were obtained using Laser

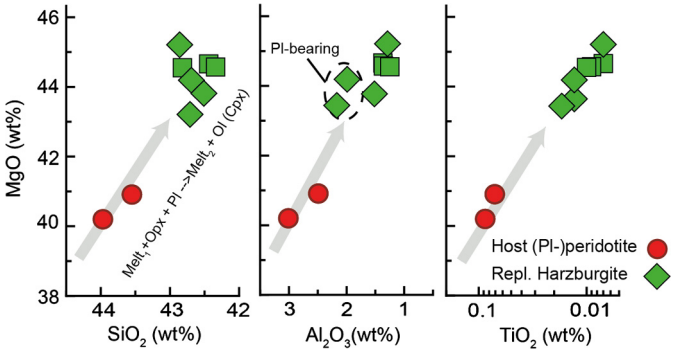

Fig. 4. Whole rock SiO_2, Al_2O_3 and TiO_2 versus MgO compositions of the Lanzo South replacive harzburgites and host Pl-peridotites. Arrow indicates the melt-rock reaction trend as expected by dissolution of orthopyroxene (and plagioclase) from the host rock and crystallization of olivine. Sharp decrease in TiO_2 suggests the depleted character of the interacting melt.

Ablation Inductively Coupled Plasma Mass Spectrometry (LA-ICP-MS) at C.N.R., Istituto di Geoscienze e Georisorse (Unità di Pavia). The probe consists of a PerkinElmerSCIEX ELAN DRC-e quadrupole mass spectrometer coupled with an UP213 deep-UV YAG Laser Ablation System (New Wave Research, Inc.). The laser was operated at a repetition rate of 10 Hz, with 213 nm wavelength and a fluence of ~9.5 J/cm^2. Helium was used as carrier gas and was mixed with Ar downstream of the ablation cell. Spot diameter was 100 microns. Data reduction was performed offline using the GLITTER software. For this study, the NIST SRM 610 synthetic glass standards was used as external standard, CaO was used as internal standard for clinopyroxene, while SiO_2 was used for olivine and orthopyroxene. Precision and accuracy of the REE concentration values were assessed through repeated analysis of the BCR2-g standard to be better than ±7% and ±10%, respectively, at the ppm concentration level.

3.4. Nd and Hf isotope analyses

Isotopic composition measurements of clinopyroxene, leaching, dissolution and column chemistry and were done at the National High Magnetic Field Laboratory, Florida State University (supplementary Table S4). The clinopyroxene separates (~200 mg, hand-picked under binocular microscope) were leached in ~5 mL 2.5N HCl and ~500 µL <30% H_2O_2 for 20–30 min at room temperature to remove any alteration products. The leached separates were rinsed several times with quartz sub-boiling distilled water. Subsequent dissolution and column chemistry was performed after procedures described in Stracke et al. (2003). Nd, and Hf isotopes were measured using the Thermofisher NEPTUNE Multi-Collector Inductively Coupled Plasma Mass Spectrometer (MC-ICP-MS). The $^{143}Nd/^{144}Nd$ ratios are corrected for mass bias using $^{146}Nd/^{144}Nd$ ratio of 0.7219 and reported relative to La Jolla standard of 0.511850. Blanks for Nd were ~10 pg. The $^{176}Hf/^{177}Hf$ ratios are corrected for mass bias using $^{179}Hf/^{177}Hf$ ratio of 0.7325 and reported relative to JMC-475 value of $^{176}Hf/^{177}Hf = 0.282150$. Blanks for Hf were <40 pg. Reproducibility of the LaJolla and JMC475 standards is similar to their in-run precision and reported in supplementary Table S6.

4. Results

Whole rock major element compositions of Pl-peridotite and spl-harzburgites reveal correlations in MgO vs. SiO_2, Al_2O_3 and TiO_2 contents, in agreement with the gradual variation in modal abundance of ol, opx and pl in these rocks (Fig. 4). Note, for instance, that the two replacive harzburgites preserving trace amount of Pl are distinguishable by relatively high Al_2O_3 contents,

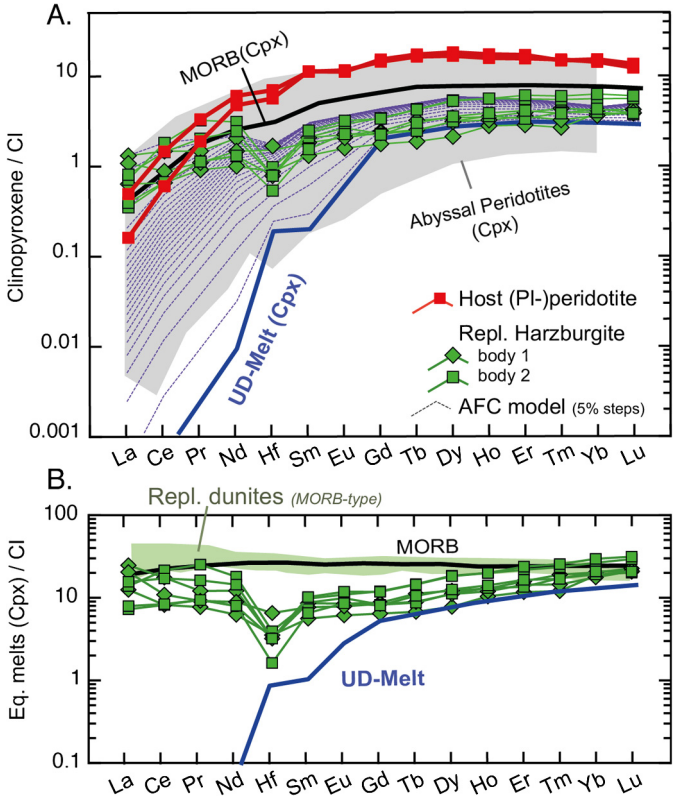

Fig. 5. A) Chondrite-normalized trace element concentrations of clinopyroxene from the Lanzo South replacive harzburgites and host Pl-peridotites. The gray field represents the cpx in abyssal peridotites (from Warren, 2012) and the black line the cpx calculated from the N-MORB composition of Gale et al. (2013). The compositions of clinopyroxene in equilibrium with melts produced by the assimilation-fractional crystallization process (AFC) are depicted in dashed, blues lines. Each step corresponds to 5% of the AFC process. UD-Melt cpx is the starting composition of cpx in equilibrium with the ultra-depleted melt in B). Parameters and equations of the AFC model in the methodological section and in Table S5. B) Chondrite-normalized trace element concentrations of melts in equilibrium with the cpx from the Lanzo South replacive harzburgites and host Pl-peridotites. The green field represents melts in equilibrium with cpx in MORB-type replacive dunites (Piccardo et al., 2007; Sanfilippo et al., 2014, 2017) from Lanzo South. Black, bold line represents the compositions of mean MORB from Gale et al. (2013). UD-Melt indicates the composition of the ultra-depleted melt as defined in this study (see text).

but have MgO and SiO_2 undistinguishable from those of the Pl-free samples. Major element compositions of ol, opx and cpx are similar amongst the different spl-harzburgites and have all highly refractory compositions, with Fo in ol ~91, and Mg# in opx and cpx ranging from 91 to 92 mol%. Spl in the Pl-free harzburgites is characterized by lower TiO_2 contents (<0.1 wt%) and Cr# (20–28), and higher Mg# (69–70) compared to the host Pl-bearing rocks (~0.6 wt%; ~57 and ~46, respectively). Interestingly, one harzburgite having high Al_2O_3 contents (LZ205) has two generations of spl. One is associated to the interstitial cpx and have low Cr# (~25); the other is included in olivine and shows Cr# similar to those of the host Pl-peridotites. Taken as a whole, TiO_2, Cr# and Mg# of the spl in the harzburgites plot in the field of spl-abyssal peridotites.

REE patterns of the cpx in replacive harzburgites show a gradual decrease in chondrite-normalized concentrations from Lu to Sm, a "high" value for Nd and a gradual decrease from Nd to La (Fig. 5). Absolute concentrations of the M- and HREE in the cpx of the Lanzo replacive harzburgites are at the low end of the field for cpx from abyssal peridotite. However, the cpx REE pattern in these replacive rocks is much flatter than patterns for residual abyssal peridotites, and LREE concentrations that are among the highest values of the abyssal peridotites field. The incompatible trace element compositions of ol and opx in the replacive

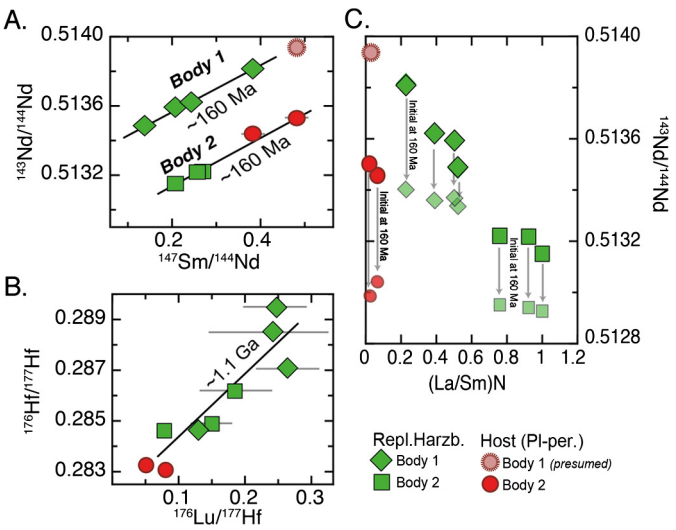

Fig. 6. Present-day $^{147}Sm/^{144}Nd$ versus $^{143}Nd/^{144}Nd$ and $^{176}Lu/^{177}Hf$ versus $^{176}Hf/^{177}Hf$ compositions of clinopyroxene. Errors (2 sigma) are indicated by gray bars. The Nd isotopic compositions for the two bodies correlates along lines yielding ages of ~160 Ma (A). These ages are in agreement with U–Pb ages of zircons from gabbroic bodies collected in other location of the Lanzo Massif (Kaczmarek et al., 2008), and indicate that the Nd systematic was totally reset during the interaction. B) The Hf isotopic compositions depict a correlation line forming apparent age of ~1.1 Ga, interpreted to be a mixing line between a highly radiogenic component and the host Pl-peridotites. AFC modeling agrees with this idea showing the different susceptibility of Nd and Hf isotope systematic during melt-rock reaction processes (see main text). C) Correlations between the C1-normalized La/Sm ratios in the replacive harzburgites Cpx and both, the present-day (solid symbols) and initial (calculated at 160 Ma and depicted in pale symbols, as indicated by the gray arrows) $^{143}Nd/^{144}Nd$ ratios. These correlations suggest a partial resetting of the Nd isotopes towards the initial composition of the host Pl-peridotites during the interaction event. The presumed composition of Pl-peridotites hosting body 1 is also reported for comparison.

harzburgites are depleted relative to that of the host Pl-peridotites (supplementary Table S3). Replacive harzburgites have ol and opx with 3.6–5.2 ppm and 110–330 ppm of Ti, respectively, whereas ol and opx in Pl-peridotites have Ti contents of ~27 ppm and ~1200 ppm. Geothermometry evaluations indicate high equilibration temperatures for both major elements and REE exchanges between cpx and opx, which yield temperatures of $990 \pm 40\,^{\circ}C$ and $1190 \pm 50\,^{\circ}C$, respectively, and similar to the abyssal peridotites from the Gakkel and SWIR ultraslow spreading ridges (Dygert and Liang, 2015; D'Errico et al., 2016).

The isotope compositions of the cpx from selected samples are reported in Fig. 6. Although the cpx from the two harzburgite bodies have similar major and trace element characteristics, they differ in Nd-isotopic composition and the two bodies from separate arrays on $^{143}Nd/^{144}Nd$ versus Sm/Nd diagram with similar slope, forming parallel error-chrones with ages of ~160 Ma (Fig. 6A). The correlations between the Nd isotopic composition and its parent daughter ratio are consistent with the published zircon ages of approximately 160 ± 2 Ma (Kaczmarek et al., 2008). Initial isotopic compositions are thereby calculated at 160 Ma, which represents the age of the replacive event. Initial ε_{Nd} for all samples are in the field of modern MORB and nearly constant for each replacive body at +14–15 and +6–8 for body one and two, respectively. On the other hand, the Hf-isotopic compositions range from MORB-like values in the host Pl-peridotites (initial $\varepsilon_{Hf} = +14$ to +19), to extreme radiogenic ratios in the replacive harzburgites (initial $\varepsilon_{Hf} = +55$ to +213) (Fig. 1).

5. Discussion

5.1. Evidence for a replacive origin

Field, textural and geochemical characteristics of studied harzburgites coherently indicate a replacive nature for the spl-harburgite bodies selected in this study. For instance, a process of annealing of the pre-existing Pl-bearing tectonites into isotropic, unfoliated harzburgites is well visible on the field (Figs. 2 and 3). This field evidence agrees with the occurrence of kinked opx and, locally, Pl partly replaced by undeformed, ol in the harzburgites (Fig. 3E). In addition, the association of interstitial cpx and sp (Fig. 3F) suggest that these minerals mainly crystallized during the last phases of the interaction process. This is further sustained by the occurrence of two generations of spl in one harzburgites preserving trace amount of pl (LZ205) (Fig. 7). Here, spl with low Cr# (~25) coexists with the interstitial cpx, whereas the spl grains included in ol preserve high Cr# (~40), similar to that of the host Pl-peridotites. These data indicate that the harzburgites formed through a reaction of the type Melt1 + Opx(±Pl ± Spl) → Melt2 + Ol(±Cpx ± Spl). Geothermometry evaluations denote that the newly formed cpx attained trace element equilibrium with the coexisting phases (opx and ol) at magmatic temperatures ($1200 \pm 100\,^{\circ}C$; see Table S3 in supplement), again consistent with a process of recrystallization and annealing of the pre-existing minerals during the replacive event.

Finally, the replacive origin of these rocks is consistent with the REE patterns of the cpx in the replacive harzburgites. Although depleted in incompatible trace elements compared to the host peridotites, the cpx in these rocks display nearly flat REE patterns, with LREE contents locally enriched compared to MREE (see Fig. 5). Given the well-known sensitivity of the L/MREE ratios during melt metasomatism in the mantle (e.g., Hellebrand and Snow, 2003; Warren, 2012), the variable LREE-MREE fractionation is attributed to the melt-peridotite interaction process. This hypothesis will be discussed in the next section together with the Nd–Hf isotopic compositions. In agreement with what previously suggested in literature (Müntener et al., 2005; Piccardo et al., 2007), we conclude that the spl-harzburgites from Lanzo South formed through a process of interaction between Pl-peridotites and migrating melts focused within decameter-scale replacive bodies.

5.2. Origin of decoupling of Nd–Hf isotopic compositions

Well-defined correlations between Hf and Os isotopes and chemical parameters indicative of degrees of melting (e.g. bulk Al_2O_3, TiO_2 in Cpx and Cr# in spinel, see Fig. 7), show that the Nd–Hf decoupling in the refractory peridotites from Gakkel ridge and Salt Lake Crater at Hawai'i results from interaction between an ancient oceanic lithosphere (having originally high ε_{Hf} and ε_{Nd} values) and MORB-like mantle melts (Bizimis et al., 2003; Stracke et al., 2011). This event would have largely reset the original Nd isotope ratio while partly preserving radiogenic Hf isotopic composition. Following this idea, the spl-harzburgites from Lanzo could represent portions of anciently depleted, refractory mantle, which partly interacted with MORB-type melts. However, this scenario is inconsistent with the evidence that these rocks are found as discrete bodies (decameter in scale) formed at the expenses of Pl-peridotites having typical DMM-like isotopic composition. In addition, the $^{176}Hf/^{177}Hf$ ratio of the cpx from the Lanzo South harzburgites does not show any correlations with other depletion indexes (Fig. 7), necessary if the extremely high Hf radiogenic signature was inherited by old depletion events (see Bizimis et al., 2003; Stracke et al., 2011). Hereafter we will show that, contrary to what has been proposed for Gakkel ridge and Salt Lake Crater peridotites, the overall trace element and isotope compositions of the

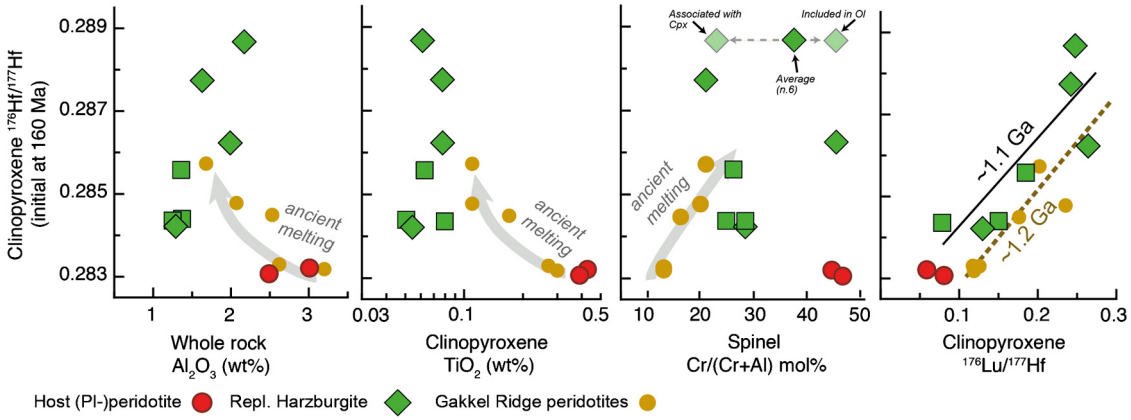

Fig. 7. Whole rock, Al_2O_3, clinopyroxene TiO_2 (wt%), spinel Cr# = [Cr/(Cr + Al)] (mol%) and clinopyroxene $^{176}Lu/^{177}Hf$ ratios versus initial clinopyroxene $^{176}Hf/^{177}Hf$ compositions (calculated at 160 Ma) of the Lanzo South replacive harzburgites and host Pl-peridotites compared to the peridotites from the Gakkel Ridge (Stracke et al., 2011). Arrow indicates the trend expected by old-depletion related by an ancient melting event. The lack of correlation between $^{176}Hf/^{177}Hf$ and depletion indexes for the Lanzo harzburgites is at odd with an origin as ancient melting residue clearly pointing to a replacive origin. Note that the $^{176}Lu/^{177}Hf$ versus $^{176}Hf/^{177}Hf$ correlation of the Lanzo harzburgites and Gakkel peridotites form subparallel lines with apparent age of 1 Ga. Although the age depicted by the Lanzo harzburgites is likely representing a mixing line, the occurrence of highly radiogenic and depleted compositions prove the existence of an asthenospheric component akin the Gakkel peridotite in the asthenospheric mantle that sourced the interacting melt.

spl-harzburgites from Lanzo South require a process of interaction between a Pl-peridotite with typical DMM-like isotopic compositions and an ultra-depleted melt with highly radiogenic Nd–Hf isotopic ratios.

The cpx from the host Pl-peridotites has REE contents (see Fig. 5) and Nd–Hf isotopic compositions (Fig. 1) indicating equilibration with melts similar to present-day MORB (see also Bodinier et al., 1991; Piccardo et al., 2007). On the other hand, the depleted composition of the replacive harzburgites requires an interaction with melts highly depleted in incompatible elements, hereafter referred to as ultra-depleted melts. Below, we show that the Nd–Hf isotope decoupling of these rocks are consistent with this interpretation.

The Nd-isotopic composition of the two bodies form parallel error-chrons with ages of ~160 Ma, coherent with the age of the replacive event (Fig. 6A). Present-day $^{143}Nd/^{144}Nd$ ratios of the cpx in the replacive harzburgites also correlate with the flattening of the REE patterns (e.g., lower La/Sm), although the Pl-peridotites do not plot into this correlation (Fig. 6). Given the dependence of the LREE in Cpx on melt-mantle interaction processes (Hellebrand and Snow, 2003; Warren, 2012), it is evident that the replacive event defined the La/Sm ratios of the cpx in the harzburgites, together with a partial reset of their Nd isotopic composition. The correlation between La/Sm and the Nd isotopes still exists if the initial $^{143}Nd/^{144}Nd$ (at 160 Ma) values are considered, but the two bodies are offset. This indicates that Nd isotopic composition of the cpxs in the harzburgites tended to be quickly reset towards that of host Pl-peridotites, whereas the fractionation in LREE was modified to different extent. Later we will show that the high La/Sm ratios in the cpx from replacive harzburgites compared to the host rock is related to the ability of a melt-rock reaction process to fractionate the most incompatible elements (DePaolo, 1981). It is noteworthy that, although we could not measure the actual Nd–Hf isotopic composition of cpx from the host rock of body 1, previous studies show Nd isotopic heterogeneity for the Lanzo South Pl-peridotites, with initial ε_{Nd} ranging from +8.7 to +12 (Bodinier et al., 1991). Hence, we can infer that high initial $^{143}Nd/^{144}Nd$ ratios of the cpx in the replacive harzburgites from body 1 are inherited from a host Pl-peridotite with a high $^{143}Nd/^{144}Nd$ values.

Unlike the Nd isotopes, the $^{176}Hf/^{177}Hf$ and $^{176}Lu/^{177}Hf$ ratios of the replacive harzburgites display a trend yielding an error-chron at ~1.1 Ga, and the present-day $^{176}Hf/^{177}Hf$ ratio does not correlate with any depletion index (Figs. 6 and 7). Given the replacive nature of the Lanzo South harzburgites, the existing correlation between $^{176}Hf/^{177}Hf$ and $^{176}Lu/^{177}Hf$ ratios is thereby likely a mixing line between a ultra-depleted, ancient component retained in the melt and the MORB-like, host Pl-peridotites. Because of the ultra-depleted nature of the migrating melts, this radiogenic source component could have been acquired by a refractory source similar to *ReLish*, with an isotopic composition similar to the refractory peridotite domains found in the asthenospheric mantle (Bizimis et al., 2003; Liu et al., 2008; Stracke et al., 2011; Byerly and Lassiter, 2014).

Based on this hypothesis, we calculated how an interaction between an ultra-depleted, radiogenic melt and a mantle peridotite affects the trace element composition and the Lu/Hf and Sm/Nd ratios of the newly formed Cpx, using assimilation-fractional crystallization equations (details on the model are in the appendix). The trace element and isotopic composition of the ultra-depleted melt was calculated by melting an ancient, refractory mantle peridotite here called *ReLish*. We modeled several scenarios to find the composition of ultra-depleted melt that better reproduces the observed cpx trace element patterns and isotopic compositions. To account for the highly radiogenic Hf isotopic composition combined with the low incompatible element concentrations of the Lanzo Cpx, the *ReLish* has to be at least 1 Ga in age. In our model, this ultra-depleted mantle was formed by melting of a 2.5 Ga-old DM-like mantle for 3% in the garnet stability field, followed by an additional 7% in the spinel stability field. The ultra-depleted melt was in turn produced by melting this *ReLish* to a low degree (5%) at low pressures. Although this model is non-unique, that part of the ancient (1 Ga) melting event that results in *ReLish* has to take place in the presence of garnet is a requirement to develop an extremely radiogenic Hf signature at reasonable melting degrees (Salters et al., 2011; Stracke et al., 2011), but continuous melting into the spinel stability field is necessary to account for the nearly flat M-to HREE patterns of the cpx in the replacive harzburgites. The assimilation-fractional crystallization (AFC) model is used to reproduce the composition of the harzburgites from body two, for which we have the Nd–Hf isotopic composition of host Pl-peridotites. The model shows that the interaction between the host Pl-peridotites and the ultra-depleted melt can reproduce the trace element compositions and the isotope decoupling of the cpx in the harzburgites. The geochemical effects of this interaction are seen in Fig. 5 and Fig. 8, where it is obvious that the cpx in equilibrium with the depleted melt shifts its isotopic composition towards that of the assimilated peridotite, but the Nd and Hf systematics will be affected to different extents. This is mainly because such an

ultra-depleted melt has much higher Hf/Nd ratio (~2.4) compared to that of the rock it is reacting with (~0.2), allowing the resulting Nd isotopic composition to be strongly constrained by that of the assimilant. In addition the Hf-isotopic contrast between the ultra-depleted melt and the assimilated peridotite is larger than the Nd-isotopic difference. In the same way, the Nd of the resulting cpx increase to a larger extent compared to the neighboring Hf and MREE (Fig. 5). As a result, an ultra-depleted melt having highly radiogenic $^{176}Hf/^{177}Hf$ and $^{143}Nd/^{144}Nd$ ratios (~0.292 and ~0.524, respectively) would experience a significant shift of its original Nd isotopic ratios towards that of the assimilant after only 1% of assimilation, whereas the Hf isotopic ratios are substantially modified only at high degrees (>25%) of interaction.

We should note, however, that the AFC model reproduces the isotopic and elemental compositions of the Lanzo South replacive harzburgites cpx for the Sm/Nd, Lu/Hf ratios and the M- to HREE contents, but fails to reproduce the extreme LREE fractionations (compare Fig. 5 and Figs. 8b and 8c). The amounts of assimilation required to preserve the high Hf–Nd decoupling (3–25%) are in fact much smaller than those required to fit the La, Ce and Pr contents in most cpxs (>25%). Extreme LREE fractionations typically characterize the interstitial cpx found in the MORB-type Lanzo South replacive dunites and were related to a second stage of interaction triggered by the entrapment of small aliquots of melts within the ol matrix during the last stage of the replacive process (Piccardo et al., 2007; Sanfilippo et al., 2014). Hence, it is obvious that the one-stage AFC model proposed here is a simplified version of the natural process that formed the Lanzo South replacive harzburgites. Despite this shortcoming, the model shows that the ultra-depleted and radiogenic signature of the melt is required to explain the refractory character and the decoupled Nd–Hf isotope compositions of the cpx in these rocks, and can nonetheless account for their high LREE contents. Given its highly radiogenic isotopic nature, this ultra-depleted melt most likely generated from a more than 1 Ga old, ultra-depleted oceanic mantle akin to the refractory, radiogenic peridotites locally found at mid-ocean ridges (Bizimis et al., 2003; Liu et al., 2008; Stracke et al., 2011; Byerly and Lassiter, 2014).

5.3. The contribution of melts from an ancient, ultra-depleted mantle to MORB magmatism

We present the first evidence that melts derived from an ancient (>1 Ga), refractory mantle were produced in the asthenosphere underlying the Jurassic mantle section of the Lanzo ophiolite. However, owing to their ultra-depleted nature, the influence of such ultra-depleted melts on the compositions of erupted MORB melts is hard to recognize. A major remaining issue is thus identifying the contribution of melts with an ultra-depleted nature to the present-day Mid Ocean Ridge magmatism. The Hf–Nd isotope variability of MORB forms a correlation aligned with a terrestrial array and points to a two source components: one with radiogenic Nd and Hf compositions, and one with unradiogenic compositions. In the simplest case this array is defined by the DM-FOZO array (Stracke, 2012). More realistically, the MORB source is a complex mixture of several mantle components (Rudge et al., 2013), of which the ancient, residual mantle peridotite represents the most depleted end member (see Byerly and Lassiter, 2014). However, a more careful look at the global dataset for MORB shows that they diverge in the Nd–Hf space, with gradually larger range of Hf compositions towards the radiogenic Nd end (Fig. 9). Salters and coauthors (2011) showed that basalts from different ridge sections depict sub-parallel Nd–Hf correlations. Nd–Hf fractionations in the presence of garnet (Blichert-Toft et al., 2005) and subsequent melting an old, refractory mantle seems a possible mechanism (Salters et al., 2011). This model requires a fortuitous combination and order of melting and mixing making this process seem unrealistic. In addition, given its refractory nature, an ancient depleted oceanic mantle would not start melting in the garnet stability field under an oceanic ridge with typical mantle potential temperature (Byerly and Lassiter, 2014). The lack of H-MREE fractionation in the cpx from the Lanzo harzburgites is consistent with this idea, and points to melting in the spinel stability field. A more realistic model entails mixing at various proportions mantle peridotites retaining variable degrees of depletion acquired at same ages (e.g., Salters et al., 2011). This model requires that large parcels of coherent mantle were preserved during a time sufficiently large to produce Nd–Hf decoupling (>1 Ga) and is compatible with the relation between the radiogenic Hf composition and the depletion in incompatible elements of the refractory mantle from the Gakkel Ridge (Stracke et al., 2011). However, while this model reproduces the observed variability of mantle sources, it does not take into consideration that erupted MORB are themself a mixture of melts derived from several mantle components with different solidi and productivities. Hence, the contribution of a melt in the mixture can substantially differ from that of the mantle component in the source (Stracke and Bourdon, 2009).

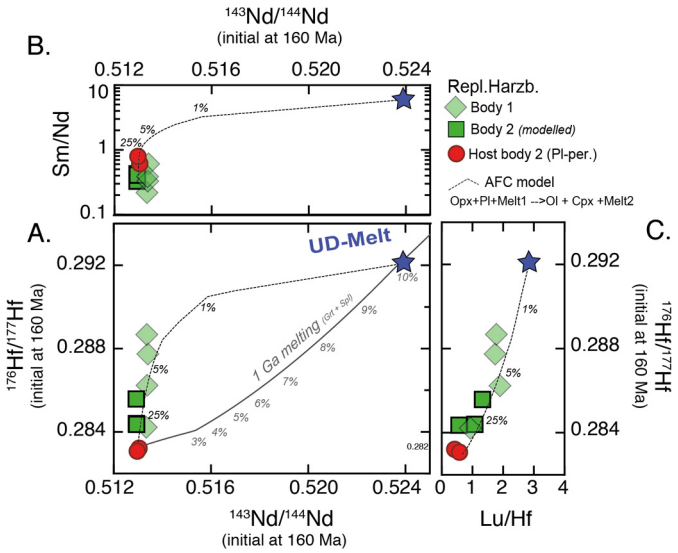

Fig. 8. Initial Nd–Hf isotope ratios A) (values recalculated at 160 Ma) and Sm/Nd B) and Lu/Hf C) ratios of the clinopyroxene in equilibrium with the melt produced by the AFC process are depicted as dashed gray lines and compared to the compositions of the clinopyroxene in the Lanzo South replacive harzburgites. The model uses the compositions of the Pl-peridotite hosting body 2. Steps corresponding to the solid mass during the AFC process are indicated by the italic numbers. Equations and parameters of the AFC model are the same as in Fig. 5 and are reported as supplementary files. The gray, solid line shows the Nd–Nf isotopic variations of a DM-like mantle (Salters and Stracke, 2004) residual from melting in the garnet (3%) plus spinel (7%) stability fields, for a depletion age of 1 Ga. The Nd–Hf isotopic compositions of the ultra-depleted melt used for the AFC process equals that of a residual DM-like mantle after 10% melting. Note that an extreme isotopic decoupling is expected at the first stage of interaction as a consequence of the higher susceptibility of Nd systematic compared to Hf, due to the much higher Hf/Nd ratio of the ultra-depleted melt compared to that of the assimilant (see Table S5).

Based on our evidence that ultra-depleted melts have been observed in a fossil section of a sub-ridge mantle, we now review this idea from a melt perspective. Owing to their depleted character, mixing ultra-depleted, radiogenic melts with melts produced by a more enriched, less radiogenic source would rapidly shift the bulk isotopic composition towards less radiogenic values. The quasi-parallel correlations observed in the Nd–Hf isotopic space at ridge segment require at least three components. A two components mixing model would equally reproduce the overall variability in the MORB field (Byerly and Lassiter, 2014). However, given the highly radiogenic and “decoupled” Nd–Hf composition

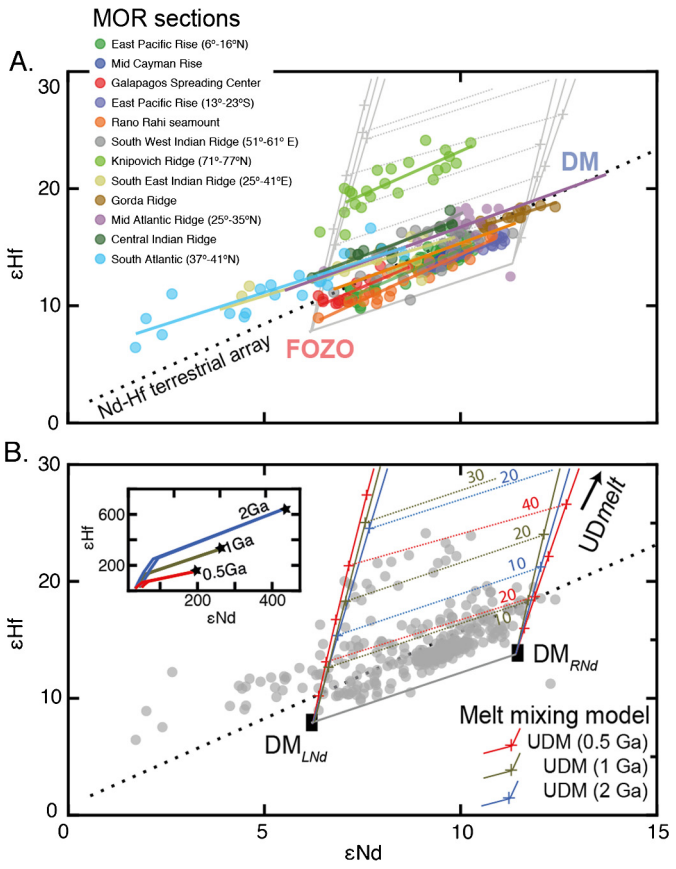

Fig. 9. A) Nd–Hf isotope variation and correlation lines of MORB from different ridge sections (data compiled from Salters et al., 2011 and references therein). The DM and FOZO compositions and the Nd–Hf global correlation lines are also indicated (see Stracke, 2012). The gray lines indicate the mixing model depicted in B). B) Nd–Hf compositions of melts produced by mixing melts from three different mantle components. UD*melt*, ultra-depleted melt as defined in this study (see Figs. 5 and 8) having Nd = 0.03 ppm and Hf = 0.07 ppm and Nd–Hf isotope ratios of a *ReLish* refractory mantle residual after ~10% partial melting, produced 0.5, 1 and 2 Ga ago (see Table S5). DM_{LNd} refers to MORB-type melts with *less* radiogenic Nd compositions from a FOZO-like mantle source ($^{143}Nd/^{144}Nd = 0.51295$; $^{176}Hf/^{177}Hf = 0.28301$); DM_{RNd} refers to MORB-type melts with radiogenic Nd compositions from a DM-like mantle ($^{143}Nd/^{144}Nd = 0.51321$; $^{176}Hf/^{177}Hf = 0.28329$). Elemental Nd and Hf compositions of these primary melts are calculated after 15% melting a DM-like source and fixed at Nd = 4.7 ppm and Hf = 1.3 ppm. Mixing lines produced by these three melt compositions are indicated by the steep lines in blue, green and red. Dashed lines depict the variability of melts produced at same proportion of UD*melt*, representing lines with constant UD*melt*/(DM_{LNd} + DM_{RNd}) ratios. These lines are parallel to the correlation lines seen in global MORB from different MOR sections.

of *ReLish*, mixing melts from two-components would necessarily produce basalts randomly distributed in the Nd–Hf space for each MOR section.

For three-end members we used ultra-depleted melts (UDM) produced by ancient, refractory peridotites (ReLish) and MORB melts formed by DM-like source having radiogenic (DM_{RNd}) and FOZO-like *less* radiogenic (DM_{LNd}) Nd isotopic signatures (Fig. 9). The extremely low incompatible element signature of the ultra-depleted melt causes a rapid shift towards the MORB field, explaining why ultra-depleted melts are yet to be seen on the seafloor. Specifically, our model shows that the sub-parallel correlation lines formed by basalts from each of the 12 MOR sections of Fig. 9 are obtained only if ultra-depleted melts have a constant contribution at a single ridge scale. Basalts from these arrays mostly retain their Nd-isotopic compositions but are "stacked" due to differences in the amount of radiogenic Hf in the ultra-depleted melt. Using the compositions of ultra-depleted melt as defined above, the global Nd–Hf variability of most MOR sections require that up to 15% of the melt budget is produced by a 1 Ga old, ultra-depleted mantle: *ReLish*. The only exception is represented by the Knipovich ridge basalts, which require up to 25% ultra-depleted melt contribution. Different ages of mantle depletion would modify the proportions of the ultra-depleted melts in Knipovich basalts to a minimum estimate of 15% and a maximum estimate of 40%, for 2 Ga and 0.5 Ga depletion ages respectively. The rest of the basalts considered in Fig. 9 would be nonetheless reproduced by a more realistic, maximum contribution of 25% of ultra-depleted melts. Independently of the contribution of *ReLish* in the erupted melts, we emphasize that the age of mantle depletion has almost no effect on the slope of the mixing lines, making this ancient, depleted mantle an ubiquitous component in the asthenosphere.

Although *Relish* experienced previous melting events, experiments showed that these depleted peridotites are still able to yield melt and melt production rates only drop significantly when Cr-diopside disappears from the solidus (Longhi, 2002). Calculations using *pMelts* also agree that depleted peridotites similar to the refractory mantle peridotites sampled at Gakkel Ridge and Salt Lake Crater in Hawai'i are still able to produce significant amounts of melt entirely in the spinel stability field (up to 10% and 5%, for the average Gakkel and Salt Lake Crater peridotites, respectively) before cpx disappears, and with a mantle potential temperature typical for MOR settings (~1350 °C) (Byerly and Lassiter, 2014).

6. Conclusions and outlook: a new model of mantle architecture

Based on geochemical and isotope compositions of decameter-scale, spl-harzburgites replacive bodies found in the southernmost portion of the Lanzo ophiolite, we found evidence that ultra-depleted melts with extremely radiogenic Hf and Nd signatures exists at a fossil Mid Ocean Ridge setting. In Lanzo, these ultra-depleted melts reactively migrated through the mantle lithosphere during the opening the nascent Ligurian Thethys Ocean, converting Pl-peridotites with typical DMM-like compositions into spl-harzburgites geochemically depleted and retaining cpx with highly decoupled Nd–Hf isotopes. The occurrence of such ultra-depleted, radiogenic melts sustains the idea that refractory, anciently depleted mantle is a ubiquitous component of the asthenosphere and may contribute to various extent to MORB petrogenesis. Mixing various proportions of variably enriched and ultra-depleted melts can explain the "stacked" arrays defined by different ridge segments in the Nd–Hf isotopic space, and allow us now to review the current model of mantle architecture.

Liu and co-workers (2008) based on the Os-isotope variations in abyssal peridotites from the Gakkel Ridge proposed that the sub-ridge mantle is highly heterogeneous, consisting of a "DM-type" asthenospheric mantle including dispersed enriched and refractory pockets. This architecture implies that ridge basalts sample the enriched and refractory pockets independent of each other. However, if these refractory mantle domains are similar to *ReLish* (Bizimis et al., 2003; Liu et al., 2008; Salters et al., 2011; Stracke et al., 2011; Byerly and Lassiter, 2014), this scenario would be inconsistent with the segment scale correlated Nd–Hf isotope variations in Fig. 9. Addition of various amounts of melts from this ancient, depleted lithosphere to more enriched melts would destroy any correlation between Nd and Hf isotopic composition that is quasi parallel to the terrestrial array in Hf–Nd isotope space. The quantitative mixing model in Fig. 9 corroborates this idea, showing that correlations in Hf–Nd isotopes are produced only if the contribution of the melts derived from *ReLish* is similar for all basaltic compositions of a single ridge segment. Such a scenario is well accommodated if *ReLish* is uniformly distributed and forms the matrix while sources that represent the most radiogenic-Nd and least radiogenic-Nd end of the ridge segment variation are discrete "pockets" (Fig. 10). The contribution of "pockets" to *ReLish*

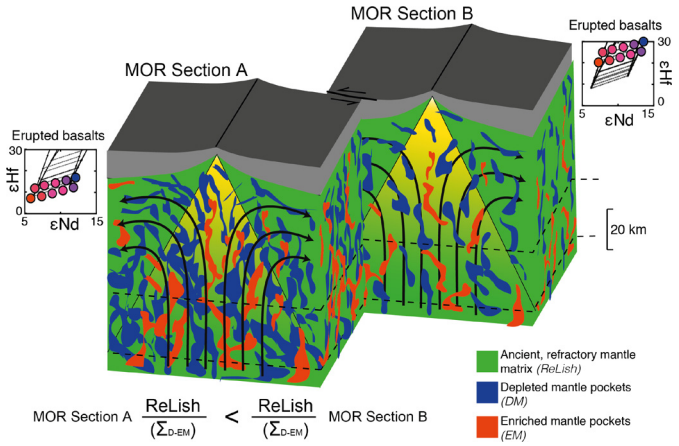

Fig. 10. Schematic representation of the asthenospheric mantle beneath two different mid-ocean ridge sections (redrawn from Liu et al., 2008). Two sections of mid-ocean ridges having different amount of ancient-refractory mantle are depicted as box diagrams separated by a transform fault. Variably radiogenic mantle pockets (ranging from depleted to enriched in trace element and isotope compositions) are randomly distributed in a matrix formed by ancient, refractory mantle survived by a long-term advection and homogenization in the asthenosphere. The amount of refractory mantle versus pockets is different in the two sections, producing erupted basalts lying on parallel Nd–Hf correlation lines. Melts erupted in each section have constant contribution of ultra-depleted melts compared to melts produced by depleted and enriched lithologies, resulting in constant ReLish/($\Sigma_{\text{D-EM}}$) ratios. The different *solidii* of the enriched and depleted lithologies are also indicated with dashed lines at different depths, defining a triangular melting region of a ∼100 km depth. Schematic plots of expected Nd–Hf basalt compositions are also indicated for each section.

is constant at the ridge scale, while the relative contribution of radiogenic-Nd pockets and least radiogenic-Nd pockets (shown as variably depleted and enriched mantle components in Fig. 10) can vary, as lithologies with different fertility are heterogeneously sampled due to difference in their solidi (Stracke and Bourdon, 2009). Magmas erupted in a ridge section are thereby distributed along parallel line in the Nd–Hf isotopic space, whereas the shift in Hf between the different MOR sections is mainly dependent on the overall amount of *ReLish* in the source (Fig. 10). This architecture is in agreement with the evidence that MORB form distinct broad isotopic provinces that reflect different domains of the upper mantle with distinctive origins and long-term evolutions (Meyzen et al., 2007) on a scale comparable to that of the ridge sections reported in Fig. 9. Conversely, the isotopic heterogeneity revealed at a ridge-scale can be caused by selective melting of variably enriched domains, believed to occur as kilometer-scale pockets within the sub-ridge mantle (Liu and Liang, 2017).

Although the occurrence of melts from refractory compositions indicates the presence of *ReLish*, an estimate of the amount of this ultra-depleted, ancient mantle is still difficult to obtain. Although highly dependent on the age of depletion, our model shows that the proportion of ultra-depleted melts in the MORB mixture can be as high as 20% for a ∼1 Ga old source. Since this ancient, refractory peridotite is significantly depleted compared to less radiogenic sources (Bizimis et al., 2003; Liu et al., 2008; Salters et al., 2011; Stracke et al., 2011; Byerly and Lassiter, 2014), its proportion in the upper mantle is likely to be even higher than what can be estimated from the composition of the basalts. Here, we prove and sustain the idea that current estimates of the trace element and isotope compositions of the upper mantle that are based on the composition of the erupted melts are biased to represent more fertile compositions (e.g., Snow et al., 1994; Salters and Dick, 2002; Salters and Stracke, 2004; Stracke and Bourdon, 2009; Stracke et al., 2011; Stracke, 2012; Rudge et al., 2013; Byerly and Lassiter, 2014). This results in a significant uncertainty in the mass of the depleted mantle (DM) end-member, which will be larger than the mass of the depleted mantle as derived from erupted MORB, if by averaging over a range of basalt compositions we assume uniform melt productivity from different sources.

Acknowledgements

We thank S. Botticchio and S. Tamburelli for their assistance in fieldwork, mineral separation and isotope analyses. Thanks to N. Menegoni and C. Perotti for their assistance in the field and for the use of structure for motion technique to reproduce the 3-D reconstruction of the outcrop. This work was financially supported by a Programma di Rilevante Interesse Nazionale (PRIN prot. 2015C5LN35) to R. Tribuzio. Part of this work was performed at the National High Magnetic Field Laboratory, which is supported by National Science Foundation Cooperative Agreement No. DMR-1157490 and the State of Florida. A.S and R.T. conceived the project and performed the preliminary field and petrological study; A.Z. performed the trace element determinations of mineral phases; A.S. and V.S. performed the geochemical modeling and wrote the text. A.S. wishes to thank A. Stracke for his precious comments on a preliminary version of this manuscript and for stimulating discussion on the origin of ReLish. This present study beneficed of comments from two anonymous reviewers.

Appendix A

Melting model Trace element concentrations are calculated using a dynamic melting model described in detail by Salters et al. (2011). We used a residual porosity of 0.1% and an amount of melt extracted at each step of 0.2%. Percentage of melting per Km was fixed at 0.3% Initial source concentrations are the depleted mantle concentrations of Salters and Stracke (2004) and the partition coefficients are from Salters and Stracke (2004) and reference therein. To produce *ReLish*, the source of the ultra-depleted melt, melting begins in the garnet stability field (∼3%) followed by further melting in the spinel stability field (see gray line in Fig. 8). The composition of ultra-depleted melt is calculated using as starting composition that of *ReLish* formed 1 Ga ago and residual after at 10% melting (3% in garnet and 7% in spinel stability fields). This *ReLish* peridotite is chemically and isotopically similar to the refractory peridotites sampled at Gakkel Ridge (Stracke et al., 2011) and is able to produce up to 10% melt with a typical mantle potential temperature of 1350° (Byerly and Lassiter, 2014). This *ReLish* mantle is melted in the spinel stability field and the trace element compositions of the accumulated melt produced at 5% melting degree is used as ultra-depleted melt to account for the observed trace and isotopic compositions of the cpx in the Lanzo South replacive harzburgites. The trace element and isotope compositions of source and of melts are given in supplementary Table S5.

Melt-rock interaction model The melt-rock interaction used to reproduce the trace element and Nd–Hf isotope compositions of the Cpx from the Lanzo replacive harzburgites is calculated using an AFC-type model based on equations 6a and 15a from DePaolo (1981), as similarly used in previous studies reproducing melt-rock reactions in the oceanic mantle (Kelemen et al., 1992; Stracke et al., 2011). An ultra-depleted melt reacts with a peridotite akin the host Pl-peridotites in Lanzo (Figs. 5, 8) at constant magma mass during reaction and mass assimilated to mass crystallized ratio ∼0.99. The interaction of the host Pl-peridotite with an ultra-depleted melt produces a highly depleted peridotite akin the replacive harzburgites from Lanzo, by preferential dissolution of orthopyroxene and plagioclase and crystallization of olivine and clinopyroxene. Trace element and isotopic compositions of the Pl-peridotite LZ11 are used as assimilant. The trace elements and

isotope composition of the cpx in equilibrium with melts produced by the AFC process is depicted in Fig. 5 and details are reported in supplementary Table S5. Partition coefficients are the same as those used for the trace element melting modeling.

Appendix B. Supplementary material

Supplementary material related to this article can be found online at https://doi.org/10.1016/j.epsl.2019.01.018.

References

Alard, O., Luguet, A., Pearson, N.J., Griffin, W.L., Lorand, J.-P., Gannoun, A., Burton, K.W., O'Reilly, S., 2005. In situ Os isotopes in abyssal peridotites bridge the isotopic gap between MORBs and their source mantle. Nature 436, 1005–1008.

Allègre, C.J., Hamelin, B., Dupré, B., 1984. Statistical analysis of isotopic ratios in MORB: the mantle blob cluster model and the convective regime of the mantle. Earth Planet. Sci. Lett. 71, 71–84.

Bizimis, M., Sen, G., Salters, V.J.M., 2003. Hf–Nd isotope decoupling in the oceanic lithosphere. Constraints from spinel peridotites from Oahu, Hawaii. Earth Planet. Sci. Lett. 217, 43–58.

Blichert-Toft, J., Agranier, A., Andres, M., Kingsley, R., Schilling, J.G., Albarède, F., 2005. Geochemical segmentation of the Mid-Atlantic Ridge north of Iceland and ridge–hot spot interaction in the North Atlantic. Geochem. Geophys. Geosyst. 6, Q01E19. https://doi.org/10.1029/2004GC000788.

Bodinier, J.L., Menzies, M.A., Thirlwall, M.F., 1991. Continental to oceanic mantle transition: REE and Sr–Nd isotopic geochemistry of the Lanzo Lherzolite Massif. J. Petrol., 191–210. Special Lherzolite Issue.

Boudier, F., Nicolas, A., 1977. Structural controls on partial melting in the Lanzo peridotites. Oreg. Dep. Geol. Miner. Ind. 96, 63–78.

Byerly, B.L., Lassiter, J.C., 2014. Isotopically ultradepleted domains in the convecting upper mantle: implications for MORB petrogenesis. Geology 42, 203–206.

Cipriani, A., Bonatti, E., Carlson, R.W., 2011. Nonchondritic ^{142}Nd in suboceanic mantle peridotite. Geochem. Geophys. Geosyst. 12 (3), Q03006. https://doi.org/10.1029/2010GC003415.

Cipriani, A., Brueckner, H.K., Bonatti, E., Brunelli, D., 2004. Oceanic crust generated by elusive parents: Sr and Nd isotopes in basalt–peridotite pairs from the Mid-Atlantic ridge. Geology 32, 657–660.

DePaolo, D.J., 1981. Trace element and isotopic effects of combined wall-rock assimilation and fractional crystallization. Earth Planet. Sci. Lett. 53, 189–202.

D'Errico, M.E., Warren, J.M., Godard, M., 2016. Evidence for chemically heterogeneous Arctic mantle beneath the Gakkel Ridge. Geochim. Cosmochim. Acta 174, 291–312.

Dygert, N., Liang, Y., 2015. Temperatures and cooling rates recorded in REE in coexisting pyroxenes in ophiolitic and abyssal peridotites. Earth Planet. Sci. Lett. 420, 151–161.

Gale, A., Dalton, C.A., Langmuir, C.H., Su, Y., Schilling, J.G., 2013. The mean composition of ocean ridge basalts. Geochem. Geophys. Geosyst. 3 (14), 489–518.

Guarnieri, L., Nakamura, E., Piccardo, G.B., Sakaguchi, C., Shimizu, N., Vannucci, R., Zanetti, A., 2012. Petrology, trace element and Sr, Nd, Hf isotope geochemistry of the North Lanzo Peridotite Massif (Western Alps, Italy). J. Petrol. 53, 2259–2306.

Hellebrand, E., Snow, J.E., 2003. Deep melting and sodic metasomatism underneath the highly oblique-spreading Lena Trough (Artic Ocean). Earth Planet. Sci. Lett. 216, 283–299.

Hofmann, A.W., 1997. Mantle geochemistry: the message from oceanic volcanism. Nature 385, 219–229.

Johnson, K.T.M., Dick, H.J.B., Shimizu, N., 1990. Melting in the oceanic upper mantle – an ion microprobe study of diopsides in abyssal peridotites. J. Geophys. Res. 95, 2661–2678.

Kaczmarek, M.A., Muntener, O., Rubatto, D., 2008. Trace element chemistry and U–Pb dating of zircons from oceanic gabbros and their relationship with whole rock composition (Lanzo, Italian Alps). Contrib. Mineral. Petrol. 155, 295–312.

Kelemen, P.B., Dick, H.J.B., Quick, J.E., 1992. Formation of harzburgite by pervasive melt/rock reaction in the upper mantle. Nature 358, 635–641.

Kelemen, P.B., Shimizu, N., Salters, V.J.M., 1995. Extraction of mid-ocean-ridge basalt from the upwelling mantle by focused flow of melt in dunite channels. Nature 375, 747–753.

Liu, B., Liang, Y., 2017. The prevalence of kilometer-scale heterogeneity in the source region of MORB upper mantle. Sci. Adv. 3, e1701872.

Liu, C.Z., Snow, J.E., Hellebrand, E., Brügmann, G., Von Der Handt, A., Büchl, A., Hofmann, A.W., 2008. Ancient, highly depleted heterogeneous mantle beneath Gakkel ridge, Arctic ocean. Nature 452, 311–316.

Longhi, J., 2002. Some phase equilibria systematics of lherzolite melting: I. Geochem. Geophys. Geosyst. 3, GC000204.

Mallick, S., Sachi-Kocher, A., Dick, H.J.B., Salters, V., 2014. Isotope and trace element insights into heterogeneity of sub-ridge mantle. Geochem. Geophys. Geosyst. https://doi.org/10.1002/2014GC005314.

McCarthy, A., Müntener, O., 2015. Ancient depletion and mantle heterogeneity: revisiting the Permian–Jurassic paradox of Alpine peridotites. Geology 43, 255–258.

Meyzen, C.M., Blichert-Toft, J., Ludden, J.N., Humler, E., Mevel, C., Albarede, F., 2007. Isotopic portrayal of the Earth's upper mantle flow field. Nature 447, 1069–1074.

Müntener, O., Piccardo, G.B., Polino, R., Zanetti, A., 2005. Revisiting the Lanzo peridotite (NW-Italy): "asthenospherization" of ancient mantle lithosphere. Ofioliti 30, 111–124.

Pelletier, L., Müntener, O., 2006. High-pressure metamorphism of the Lanzo peridotite and its oceanic cover, and some consequences for the Sesia-Lanzo zone (northwestern Italian Alps). Lithos 90, 111–130.

Picazo, S., Müntener, O., Manatschal, G., Bauville, A., Karner, G., Johnson, C., 2016. Mapping the nature of mantle domains in Western and Central Europe based on clinopyroxene and spinel chemistry: evidence for mantle modification during an extensional cycle. Lithos 266–267, 233–263.

Piccardo, G.B., Zanetti, A., Muntener, O., 2007. Melt/peridotite interaction in the Southern Lanzo peridotite: field, textural and geochemical evidence. Lithos 94, 181–209.

Quick, J.E., 1981. The origin and significance of large, tabular dunite bodies in the Trinity peridotite, northern California. Contrib. Mineral. Petrol. 78, 413–422.

Rudge, J.R., Maclennan, J., Stracke, A., 2013. The geochemical consequences of mixing melts from a heterogeneous mantle. Geochim. Cosmochim. Acta 114, 112–143.

Salters, V.J.M., Dick, H.J.B., 2002. Mineralogy of the mid-ocean-ridge basalt source from neodymium isotopic composition of abyssal peridotites. Nature 418, 68–72.

Salters, V.J.M., Dick, H.J.B., 2011. Ultra depleted mantle at the Gakkel Ridge based on Hafnium and Neodymium isotopes. Eos Trans. AGU, Fall Meeting Suppl. 92. V41G-02.

Salters, V.J.M., Mallick, S., Hart, S.R., Langmuir, C.H., Stracke, A., 2011. Domains of depleted mantle; new evidence from hafnium and neodymium isotopes. Geochem. Geophys. Geosyst. https://doi.org/10.1029/2011GC003617.

Salters, V.J.M., Stracke, A., 2004. Composition of the depleted mantle. Geochem. Geophys. Geosyst. 5, Q05B07. https://doi.org/10.1029/2003GC000597.

Sanfilippo, A., Tribuzio, R., Ottolini, L., Hamada, M., 2017. Water, lithium and trace element compositions of olivine from replacive mantle dunites (Lanzo South massif, Western Alps): implications for melt extraction at Mid Ocean Ridges. Geochim. Cosmochim. Acta 214, 51–72.

Sanfilippo, A., Tribuzio, R., Tiepolo, M., 2014. Mantle–crust interaction in the oceanic lithosphere: constraints from minor and trace elements in olivine. Geochim. Cosmochim. Acta 141, 423–439.

Shorttle, O., Maclennan, J., 2011. Compositional trends of Icelandic basalts: implications for short length scale lithological heterogeneity in mantle plumes. Geochem. Geophys. Geosyst. 12, Q11008. https://doi.org/10.1029/2011gc003748.

Snow, J.E., Hart, S.R., Dick, H.J.B., 1994. Nd and Sr isotope evidence linking mid-ocean-ridge basalts and abyssal peridotites. Nature 371, 57–60.

Sobolev, A.V., Shimizu, N., 1993. Ultra-depleted primary melt included in an olivine from the Mid-Atlantic ridge. Nature 363, 151–154.

Stracke, A., 2012. Earth's heterogeneous mantle: a product of convection-driven interaction between crust and mantle. Chem. Geol. 330–331, 274–299.

Stracke, A., Bizimis, M., Salters, V.J.M., 2003. Recycling of oceanic crust: quantitative constraints. Geochem. Geophys. Geosyst. 4, 8003. https://doi.org/10.1029/2001GC000223.

Stracke, A., Bourdon, B., 2009. The importance of melt extraction for tracing mantle heterogeneity. Geochim. Cosmochim. Acta 73, 218–238.

Stracke, A., Snow, J.E., Hellebrand, E., von der Handt, A., Bourdon, B., Birbaum, K., Gunther, G., 2011. Abyssal peridotite Hf isotopes identify extreme mantle depletion. Earth Planet. Sci. Lett. 308, 359–368.

Warren, J., 2012. Global variations in abyssal peridotite compositions. Lithos 248–251, 193–219.

Warren, J.M., Shimizu, N., Sakaguchi, C., Dick, H.J.B., Nakamura, E., 2009. An assessment of upper mantle heterogeneity based on abyssal peridotite isotopic compositions. J. Geophys. Res. 114, 36.

White, W.M., Hofmann, A.W., 1982. Mantle heterogeneity and isotopes in oceanic basalts. Nature 295, 363–364.

Zindler, A., Hart, S., 1986. Chemical geodynamics. Annu. Rev. Earth Planet. Sci. 14, 493–571.